Surface-projected spectral densities in crystal with planar defects

1998 J. Phys.: Condens. Matter 10 8619

(http://iopscience.iop.org/0953-8984/10/39/001)

J. Phys.: Condens. Matter **10** (1998) 8619–8628. Printed in the UK PII: S0953-8984(98)93771-7

Surface-projected spectral densities in crystal with planar defects

E S Syrkin and A V Tutov†

B I Verkin Institute for Low Temperature Physics and Engineering, 310164 Kharkov, Ukraine

Received 29 April 1998, in final form 24 June 1998

Abstract. The full description of the energy spectrum is given for a fcc crystal with a passive interface. Calculations are performed in the framework of lattice dynamics, taking into account nearest-neighbour central interactions. The exact solutions for the projected densities of shear phonons are obtained, and both low-frequency and high-frequency shear waves localized at the interface are described analytically. It is shown that the full set of the eigen-solutions of the boundary-value problem is divided into two classes—symmetrical and antisymmetrical about the plane of the defect. The appearance of the localized interface wave is associated with singularities of the projected density of states at the corresponding edge of the bulk band for a certain value of the two-dimensional wave vector.

1. Introduction

The presence of a planar crystal defect substantially changes the spectrum of quasiparticle excitations and can lead to localized vibrations whose amplitude decreases from the defect towards the bulk of the crystal. The energy spectrum of the surface long-wavelength excitations has been widely investigated by means of Brillouin scattering (BS). First applied to optically transparent materials, BS soon became an effective instrument for the study of diverse surface excitations such as surface acoustic and spin waves in thin films, and at interfaces of multilayered materials. BS investigation has been particularly successful in the study of surface waves and resonances, and 'leaky' and pseudosurface vibrations of the continuous spectrum [1–6].

Two main mechanisms are known to be responsible for the inelastic scattering of light: the elasto-optical coupling caused by the modulation of the dielectric constant ϵ of the medium (mainly for optically transparent materials), and the 'ripple' mechanism which is dominant for opaque crystals. The latter mechanism makes it possible to observe vibrations associated with the surface (actually the waves at the planar crystal defect). The theory of BS from the surface thermally excited acoustical 'ripple' involves the response function of the scattering surface wave and its projected density of states [7]. Choosing the light scattering plane, and so determining the two-dimensional vector for the surface wave, one can separate shear horizontal (SH) waves from sagittally polarized waves for some crystallographic directions [8], and study the features of each spectrum of the surface excitations.

† Now on leave; current address: Department of Physics and Astronomy, University of California, Irvine, CA 92697-4575, USA.

0953-8984/98/398619+10$19.50

The dispersion of the localized elastic modes, as well as the power spectrum, can be probed in any wavelength region by means of electron energy-loss spectroscopy and low-energy light-atom He scattering [9, 10].

Here we present an elegant and effective procedure for the calculation of the projected density of the SH interface phonons using the Jacobi matrix method [11, 12] (the recursion method). The method does not involve the use of Bloch's theorem or the band structure of phonons in any way, and so can be applied to complicated (reconstructed) surfaces. We choose a certain model of the defect to describe the excitations localized at the interface between two fcc crystals, and find the change of the bulk band caused by the defect for the SH vibrations analytically.

2. Methods

The basic characteristics of the elastic surface waves, the cross sections of the BS, are described by means of the so-called projected density of phonon states $\varrho(\boldsymbol{\kappa}, \omega)$ (PDPS). For instance, the expression for the mean square displacement power spectrum involves the factor $\varrho(\boldsymbol{\kappa}, \omega)$ directly, and has the form [7, 13]

$$\langle v_\alpha^2(\boldsymbol{\kappa}, \omega, r_\perp)\rangle = \frac{k_B T}{h\omega} \sum_j |\boldsymbol{e}_\alpha(\boldsymbol{\kappa}, \omega_j, r_\perp)|^2 \varrho(\boldsymbol{\kappa}, \omega_j)$$

(the two-dimensional wave vector $\boldsymbol{\kappa}$ in the defect plane is introduced, $r_\perp$ determines the normal distance from the defect plane; $k_B T/h\omega$ is the high-temperature thermal factor, j is the branch index, and $\boldsymbol{e}_\alpha(\boldsymbol{\kappa}, \omega_j, r_\perp)$ are the polarization vectors divided by the corresponding frequency value $\sqrt{\omega_j}$).

A special method for PDPS calculation was introduced in papers [14] (see also [15]). We describe the main items of the method associated with the PDPS below.

The dynamics of the crystal lattice in harmonic approximation is based on the following equation:

$$\frac{\partial \chi_i(\boldsymbol{R}, t)}{\partial t^2} = -\sum_{\boldsymbol{R}'} L_{ik}(\boldsymbol{R}, \boldsymbol{R}')\chi_k(\boldsymbol{R}', t) \tag{1}$$

where $\chi_k(\boldsymbol{R}, t)m^{1/2}(\boldsymbol{R})$ is the kth component of the vector giving the displacement of the atom from its equilibrium position; $m(\boldsymbol{R})$ is the mass of the atom in the $\boldsymbol{R}$ position;

$$L_{ik}(\boldsymbol{R}, \boldsymbol{R}') = m^{1/2}(\boldsymbol{R})m^{1/2}(\boldsymbol{R}')A_{ik}(\boldsymbol{R}, \boldsymbol{R}')$$

and the matrix $A_{ik}(\boldsymbol{R}, \boldsymbol{R}')$ contains the interaction constants for the atoms.

Let us consider the defect which preserves the crystal periodicity in a certain crystal plane (say, in the (001) plane), i.e. we assume

$$m(\boldsymbol{R}) = m \qquad L_{ik}(\boldsymbol{R}, \boldsymbol{R}') = L_{ik}(x - x', y - y', zz'). \tag{2}$$

Searching for the solution of equation (1) in the form

$$\chi_i(\boldsymbol{R}, t) = \chi_i(z)\exp(\mathrm{i}(k_x x + k_y y) - \mathrm{i}\omega t) \tag{3}$$

we obtain the following equation:

$$\sum_{\boldsymbol{\kappa}, z'} (\lambda\delta_{ik}\delta_{zz'} - C_{ik}(\boldsymbol{\kappa}; zz'))\chi_i(z') = 0 \tag{4}$$

where $\boldsymbol{\kappa}$ is the two-dimensional wave vector with the components k_x, k_y; $\lambda = \omega^2$; and

$$C_{ik}(\boldsymbol{\kappa}; zz') = \sum_{x,y} L_{ik}(z, z'; x, y)\exp(-\mathrm{i}(k_x x + k_y y)). \tag{5}$$

When the planar defect disturbs a finite number of crystal layers, we can write the self-adjoint operator $\hat{C}(\boldsymbol{\kappa})$ in the space H of the atom displacements in the form

$$\hat{C}(\boldsymbol{\kappa}) = \hat{C}^{(0)}(\boldsymbol{\kappa}) + \hat{\Lambda}(\boldsymbol{\kappa}) \tag{6}$$

where the linear operator $\hat{\Lambda}(\boldsymbol{\kappa})$ describes the presence of the planar defect, and has a finite number of non-zero matrix elements in coordinate space; the operator $\hat{C}_{ik}(\boldsymbol{\kappa}; zz')$ transforms into $\hat{C}^{(0)}_{ik}(\boldsymbol{\kappa}; z - z')$ in the case of the ideal crystal.

Let us choose the normalized arbitrary vector $\boldsymbol{h}$ in the space H and construct the row

$$\boldsymbol{h}, \hat{C}\boldsymbol{h}, \hat{C}^2\boldsymbol{h}, \ldots.$$

Orthonormalizing the row, we get the following set:

$$\boldsymbol{h}^{(0)}, \boldsymbol{h}^{(1)}, \boldsymbol{h}^{(2)}, \ldots \tag{7}$$

which becomes the basis of some subspace H^h of the Hilbert space H. The subspace H^h is associated with the initial vector $\boldsymbol{h}$. The self-adjoint operator $\hat{C}(\boldsymbol{\kappa})$ creates the operator $\hat{C}^h(\boldsymbol{\kappa})$ in the subspace H^h, and the matrix of the operator $\hat{C}^h(\boldsymbol{\kappa})$ has the form of the three-diagonal Jacobi matrix in the basis (7), i.e. $\hat{C}^h_{ik} = (h_i, \hat{C}h_k) = 0$ for $|i - k| \geqslant 2$.

The Jacobi matrix possesses the following property: its elements (a_n: diagonal; and b_n: the non-diagonal) tend to certain constant values when $n \to \infty$. For instance, if the spectrum of the operator $\hat{C}$ is continuous, the operator $\hat{C}$ is defined over a finite energy interval $[\lambda_1(\boldsymbol{\kappa}), \lambda_2(\boldsymbol{\kappa})]$, and its spectral density $\varrho(\lambda, \boldsymbol{\kappa})$ satisfies the condition

$$\int_{\lambda_1}^{\lambda_2} |\ln \varrho(\lambda, \boldsymbol{\kappa})| \, \mathrm{d}\lambda < \infty \tag{8}$$

then the limiting values of the matrix elements are

$$a = \lim_{n\to\infty} a_n = \frac{1}{2}[\lambda_1(\boldsymbol{\kappa}) + \lambda_2(\boldsymbol{\kappa})] \qquad b = \lim_{n\to\infty} b_n = \frac{1}{4}[\lambda_2(\boldsymbol{\kappa}) - \lambda_1(\boldsymbol{\kappa})]. \tag{9}$$

The spectral density corresponding to the Jacobi matrix for which the first $2n + 1$ matrix elements differ from their limiting values and the remaining elements are equal to their limiting values can be written in the form

$$\varrho(\lambda, \boldsymbol{\kappa}) = \frac{1}{\pi} \frac{\operatorname{Im} K(\lambda, \boldsymbol{\kappa})}{|P_{n+1}(\lambda, \boldsymbol{\kappa}) - b_n P_n(\lambda, \boldsymbol{\kappa}) K(\lambda, \boldsymbol{\kappa})|^2}. \tag{10}$$

Here $P_n(\lambda, \boldsymbol{\kappa})$ are the nth-degree polynomials in λ, which satisfy the following conditions:

$$b_n P_{n+1}(\lambda, \boldsymbol{\kappa}) = (\lambda - a_n) P_n(\lambda, \boldsymbol{\kappa}) - b_{n-1} P_{n-1}(\lambda, \boldsymbol{\kappa}) \tag{11}$$

under the initial conditions $P_{-1}(\lambda, \boldsymbol{\kappa}) = 0$, $P_0(\lambda, \boldsymbol{\kappa}) = 1$. The function $K(\lambda, \boldsymbol{\kappa})$ in equation (11) is a continued fraction corresponding to the Jacobi matrix with the elements equal to their limiting values. If conditions (9) are satisfied, the continued fraction $K(\lambda, \boldsymbol{\kappa})$ has the form

$$K(\lambda, \boldsymbol{\kappa}) = \frac{8}{[\lambda_2(\boldsymbol{\kappa}) - \lambda_1(\boldsymbol{\kappa})]^2} \left[\lambda - \frac{1}{2}[\lambda_1(\boldsymbol{\kappa}) + \lambda_2(\boldsymbol{\kappa})] \pm \mathrm{i}\sqrt{(\lambda - \lambda_1(\boldsymbol{\kappa}))(\lambda_2(\boldsymbol{\kappa}) - \lambda)} \right]. \tag{12}$$

In the next section we apply the above method to the analysis of the SH interface phonons in fcc crystal.

3. Results

While analysing the vibrations at any defect in a crystal on the basis of the crystal lattice dynamics, taking into account explicitly the discreteness of the crystal structure, we must consider the finite size of the defect, which cannot be smaller than the atomic spacing. As a result, the vibrations localized at the defect acquire characteristics which cannot be studied in a continual description of the vibrations. For instance, while studying the planar defect in a crystal we can encounter vibrations in which opposite banks of the planar defect vibrate in antiphase. In our opinion such peculiarities are associated with the discreteness of the crystal and with the finite size of the defect rather than with its structure. In this connection we demonstrate the peculiarities of the localized vibrations by using the following model of the planar defect. In this model the defect can be regarded as a coherent contact between two crystalline half-spaces connected through atomic interactions which differ from the atomic interactions in each half-space. Such a model describes the interface qualitatively, and was used earlier both to emphasize the interface contribution to the surface wave properties [16, 17] and the agreement of the form of the boundary conditions in the long-wavelength limit [18], and to show the peculiarities of the interfilm exchange in magnetic multilayers [19].

We study the model of a one-atom fcc crystal lattice with short-range interactions between nearest neighbours. The crystal structure under consideration satisfies the conditions of translation and rigid-rotation invariance, and is mechanically stable [20]. We choose the axes along the [100], [010], [001] crystallographic directions and fix the (001) plane. Later, we will characterize the displacement with a scalar function $|n|m\rangle$ where n refers to the number of the atomic layer counting from the fixed plane, and m is the value of the displacement of the whole atomic layer.

Let the constant of the central interactions between the nearest neighbours in the fcc crystal in the planes of the opposite banks of the interface β differ from the force constant α in the crystals; we assume that the interface passes between two adjacent (001) atomic planes. Then the quantity $\epsilon = 1 - \beta/\alpha$ characterizes the relative change in the force interaction near the interface. An enhancement (suppression) of the coupling between two planes in the defect region corresponds to $\epsilon < 0$ ($\epsilon > 0$). As we study one-component pure shear waves of horizontal polarization, we assume the scalar model of the crystal dynamics without loss of generality. Waves of horizontal polarization split off the waves polarized in the sagittal plane propagating along a direction of high symmetry on a surface of high symmetry [8]. That is why we have analogous results for shear horizontal waves in the framework of the vector model. The translation invariance persists in the plane (001). We introduce a Fourier transformation in the plane (001), and obtain the matrix of interaction constants for the atoms in the following form (the defect planes are chosen to be the planes $n = 0, n = 1$; index n labels the planes):

$$\begin{aligned}
&C_{nn}(\boldsymbol{\kappa}) = 12 - 4\cos k_x \cos k_y \equiv p \qquad i \neq 0, 1 \\
&C_{nn+1}(\boldsymbol{\kappa}) = -\frac{1}{2}(\cos k_x + \cos k_y) \equiv -4s \qquad i \neq 0, 1 \\
&C_{00}(\boldsymbol{\kappa}) = C_{11}(\boldsymbol{\kappa}) = p - 4\epsilon \\
&C_{01}(\boldsymbol{\kappa}) = C_{10}(\boldsymbol{\kappa}) = -4(1-\epsilon)s \\
&C_{nn'}(\boldsymbol{\kappa}) = 0 \qquad |n - n'| \geqslant 2.
\end{aligned} \tag{13}$$

The eigen-solutions localized at the interface can be divided into two types—symmetrical (s) and antisymmetrical (a) vibrations [16, 17]. Displacements of the layers closest to the plane of the defect coincide for the symmetrical vibrations, and the displacements have

opposite signs for the antisymmetrical vibrations. Vibrations of both types correspond to the energies lying above, as well as below, the continuous energy spectrum of the bulk vibrations.

Such a division of the displacement space into two types of vibration (actually into two subspaces of displacements) is natural if the defect possesses a centre of symmetry, and, in fact, was applied in the study of the dynamics of the one-dimensional chain with a local 'symmetrical' defect [21]. In our model, the set of the two types of vibration is complete.

We choose the normalized initial vectors corresponding to each type of vibration as the sum of and the difference between the displacements of the opposite banks of the defect.

(1) Symmetrical waves. The initial vector has the form

$$h_s = \frac{1}{\sqrt{2}}(|0|1\rangle + |1|1\rangle) \tag{14}$$

where the first number corresponds to the number of the crystal plane parallel to the defect's, and the second number shows the value of the displacement (in our case, only the sign matters). The numbering (first number) increases toward the bulk of the crystal. Applying procedure (7) to the chosen initial vector (14), we obtain the corresponding Jacobi matrix whose elements have the form

$$J_{00} = p - \theta_s \qquad J_{ii} = p \qquad J_{ii+1} = -4s \tag{15}$$

where

$$\theta_s = 4[\epsilon(1-s) + s].$$

We use the notation (13) for the quantities p and s.

Note that the choice of initial vector (14) ensures that the J-matrix elements show rapid asymptotic behaviour starting from the first step.

(2) Antisymmetrical waves. The initial vector has the form

$$h_a = \frac{1}{\sqrt{2}}(|0|1\rangle - |1|1\rangle). \tag{16}$$

Applying procedure (7) to the chosen initial vector (16) we obtain the corresponding Jacobi matrix whose elements have the form

$$J_{00} = p - \theta_a \qquad J_{ii} = p \qquad J_{ii+1} = b \tag{17}$$

where

$$\theta_a = 4[\epsilon(1+s) - s].$$

The choice of initial vector (16) also ensures that the J-matrix elements show asymptotic values starting from the first step.

The form of the J-matrices (15), (17) makes it possible to calculate *exactly* the spectral densities corresponding to the initial vectors (14), (16) in our model. So, the projected spectral densities are

$$\varrho_{s\,(a)}(\lambda, \boldsymbol{\kappa}) = \frac{1}{2\pi\theta_{s\,(a)}} \frac{\sqrt{\lambda - \lambda_1(\boldsymbol{\kappa})}\sqrt{\lambda_2(\boldsymbol{\kappa}) - \lambda}}{\lambda - \lambda_{*s\,(a)}(\boldsymbol{\kappa})} \tag{18}$$

where

$$\lambda_{*s\,(a)}(\boldsymbol{\kappa}) = \lambda_1(\boldsymbol{\kappa}) - \frac{(\theta_{s\,(a)} - 4s)^2}{\theta_{s\,(a)}} = \lambda_2(\boldsymbol{\kappa}) - \frac{(\theta_{s\,(a)} + 4s)^2}{\theta_{s\,(a)}}.$$

The total projected spectral density (the distribution function of the energies with a fixed value of $\boldsymbol{\kappa}$) is the half-sum of the symmetrical and antisymmetrical spectral densities:

$$\varrho(\lambda, \boldsymbol{\kappa}) = \frac{1}{2}\left[\varrho_s(\lambda, \boldsymbol{\kappa}) + \varrho_a(\lambda, \boldsymbol{\kappa})\right]. \tag{19}$$

The distribution function of the energies which corresponds to the vibrations of the atom in the defect area is given by the equation

$$\varrho(\lambda) = \int \varrho(\lambda, \boldsymbol{\kappa})\ \mathrm{d}\boldsymbol{\kappa} \tag{20}$$

and it determines the thermodynamical properties of the crystal.

The edges of the bulk vibrational band in the model under consideration have the form

$$\lambda_1 = p - 8s \qquad \lambda_2 = p + 8s. \tag{21}$$

Searching for a localized solution in the form $\chi(n) \sim q^n$, we can obtain the damping parameters q of the symmetrical and antisymmetrical waves [16, 17]:

$$\begin{aligned} q_s &= \frac{s}{s + \epsilon(1-s)} \\ q_a &= \frac{s}{\epsilon(1+s) - s}. \end{aligned} \tag{22}$$

In the case where $0 < \epsilon < 1$ (suppression of the atomic interaction), vibrations of the symmetrical type corresponding to energies below the continuous spectrum exist for any value of the two-dimensional wave vector $\boldsymbol{\kappa}$. Vibrations of the antisymmetrical type with energies below the continuous spectrum edge correspond to certain values of $s > s_\downarrow$, where $s_\downarrow = \epsilon/4(2+\epsilon)$. The damping parameters are positive: $q_s, q_a > 0$. The energies of both types of interface vibration are the following:

$$\begin{aligned} \lambda_s &= \lambda_1 - \frac{2\epsilon^2(1-s)^2}{s + \epsilon(1-s)} \\ \lambda_a &= \lambda_1 - \frac{2\left[2s - \epsilon(1+s)\right]^2}{\epsilon(1+s) - s}. \end{aligned} \tag{23}$$

When $\epsilon < 0$ (enhancement of the atomic interaction), vibrations of the antisymmetrical type corresponding to energies above the continuous spectrum exist for any value of the two-dimensional wave vector $\boldsymbol{\kappa}$. Vibrations of the symmetrical type with energies above the continuous spectrum edge correspond to certain values of $s > s_\uparrow$, where $s_\uparrow = |\epsilon|/4(2+|\epsilon|)$. The damping parameters are negative: $q_s, q_a < 0$. The energies of both types of localized vibration are the following:

$$\begin{aligned} \lambda_s &= \lambda_2 + \frac{2\epsilon^2(1+s)^2}{s - \epsilon(1+s)} \\ \lambda_a &= \lambda_2 + \frac{2\left[2s + \epsilon(1-s)\right]^2}{\epsilon(s-1) - s}. \end{aligned} \tag{24}$$

As ϵ decreases from its limiting value $\epsilon = 1$ to $\epsilon = 0$, the dispersion curves of the low-energy interface vibrations corresponding to both symmetrical and antisymmetrical modes approach the lower edge of the continuous spectrum, $\lambda_1(\boldsymbol{\kappa})$. At a fixed value of the parameter ϵ only symmetrical vibrations exist in the extreme long-wavelength region. When the parameter ϵ becomes negative, we have the opposite situation: the dispersive curves move away from the upper bulk edge $\lambda_1(\boldsymbol{\kappa})$ with the increase of ϵ, and only antisymmetrical vibrations exist for an arbitrary value of $\boldsymbol{\kappa}$ (figure 1).

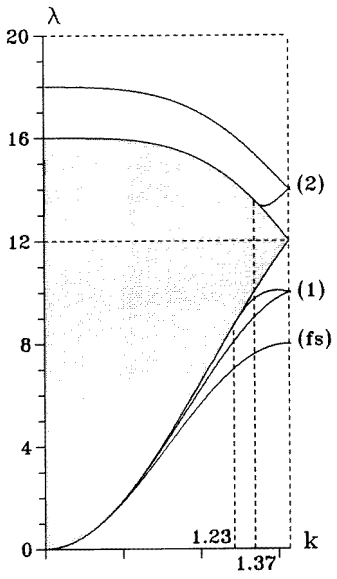

Figure 1. The phonon spectrum of the fcc lattice with the passive interface (direction ΓX of the two-dimensional Brillouin zone is chosen; $\boldsymbol{\kappa} = (k, k)$); branches of localized vibrations: (fs) $\epsilon = 1$ (free surface); (1) $\epsilon = 0.5$; (2) $\epsilon = -0.5$.

The behaviour of the PDPS for each type of vibration is shown in figure 2.

The free-surface PDPS is illustrated in figure 2(a). There is only one localized state in this case (curve (fs) in figure 1), and $\varrho_s = \varrho_a$. When $\boldsymbol{\kappa}$ equals zero, we have a singularity (ϱ tends to infinity) at the lower edge of the bulk band. The means that the localized state splits off from the bulk band without any threshold. While the wave vector increases, the area under the curve $\varrho(\lambda, \boldsymbol{\kappa})$ decreases, and the energy transfers to the localized state.

Generally, the weight of the localized state can be calculated exactly:

$$\mu_j(\boldsymbol{\kappa}) = \sum_n \left[P_n^2(\lambda, \boldsymbol{\kappa})\right]^{-1} = 1 - q_j^2 \tag{25}$$

where the subscript $j = s, a$ indicates the type of the vibration. The area under the curve $\varrho_j(\lambda, \boldsymbol{\kappa})$ is determined by the integral over the bulk band, which is equal to

$$I_j(\boldsymbol{\kappa}) = \int_{\lambda_1}^{\lambda_2} \varrho_j(\lambda, \boldsymbol{\kappa})\ \mathrm{d}\lambda = q_J^2. \tag{26}$$

Thus the conservation law can be presented as

$$\int_{\lambda_1}^{\lambda_2} \varrho_j(\lambda, \boldsymbol{\kappa})\ \mathrm{d}\lambda + \mu_j(\boldsymbol{\kappa}) = 1 \tag{27}$$

for any two-dimensional wave vector $\boldsymbol{\kappa}$. In the short-wavelength limit $\boldsymbol{\kappa} = (\pi/2, \pi/2)$, the spectral densities tend to zero, and the weight of the localized state is unity; the damping parameter equals zero at this point, so the interface vibrations are localized at the defect layers only.

For the case where $0 < \epsilon < 1$ (suppression of the atomic interactions in the defect area), PDPS of both types of vibration are shown in figure 2(b). There are two low-energy localized states now (corresponding to curves (1) in figure 1), which do not occur simultaneously for

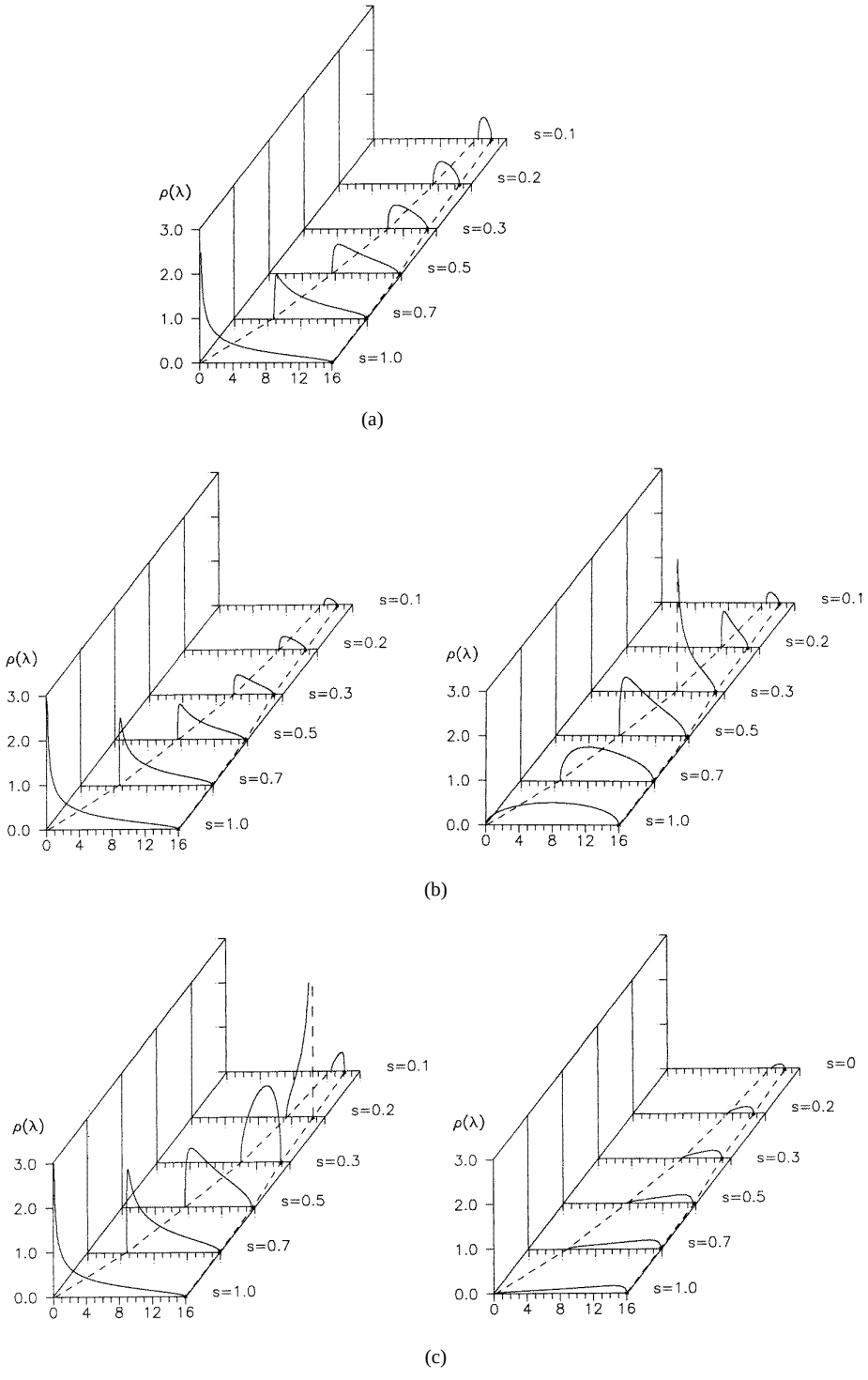

Figure 2. (a) The PDPS for the (001) free surface of the fcc lattice, $\varrho_s(\lambda, k) = \varrho_a(\lambda, k)$. (b) PDPS for the case where $\epsilon = 0.5$. $\varrho_s(\lambda, k)$: symmetrical vibrations (left); $\varrho_a(\lambda, k)$: antisymmetrical vibrations (right). (c) PDPS for the case where $\epsilon = -0.5$. $\varrho_s(\lambda, k)$: symmetrical vibrations (left); $\varrho_a(\lambda, k)$: antisymmetrical vibrations (right).

the arbitrary wave vector $\boldsymbol{\kappa}$; see equation (23). The symmetrical vibrations split off from the bulk band when $\boldsymbol{\kappa} = 0$ without a threshold, and we have a singularity of the PDPS for these waves in the long-wavelength limit. Then the weight of the symmetrical localized state increases, and reaches its maximum value at the edge of the two-dimensional Brillouin zone; meanwhile the contribution to the band decreases to zero until the point $\boldsymbol{\kappa} = (\pi/2, \pi/2)$ is reached. The antisymmetrical vibrations do not share the localized weight (26) until the critical point $\boldsymbol{\kappa}_{\downarrow}$ is reached; $I_a = 1$ everywhere in the area of larger wavelengths. The singularity at the point $\boldsymbol{\kappa}_{\downarrow}$ shows that the antisymmetrical localized waves split off from the bulk band, and further on the weight of the localized state increases. The behaviour of the antisymmetrical waves at the Brillouin zone boundary is the same as for the symmetrical waves: the vibrations are localized at the defect layers and do not penetrate into the bulk of the crystals.

For $\epsilon < 0$ (enhancement of the atomic interaction in the defect area), PDPS for each of the types of vibration are illustrated in figure 2(c). We have two localized states (corresponding to curves (2) in figure 1) with energies above the edge of the bulk band $\lambda_2(\boldsymbol{\kappa})$, and neither type of vibration occurs for the arbitrary wave vector $\boldsymbol{\kappa}$; see equation (24). The antisymmetrical localized vibrations exist for any wave vector $\boldsymbol{\kappa}$, and the PDPS do not have any singularity, either on the edges or inside the bulk band. The behaviour of the antisymmetrical vibrations is as follows: localized waves have more weight the further the localized curve is situated from the bulk band, and so increase in weight with the increase of $|\epsilon|$; the value of the wave vector matters—the weight of the localized wave achieves its maximum for short wavelengths. The symmetrical localized vibrations can occur for short enough wavelengths—starting from the critical wave vector $\boldsymbol{\kappa}_{\uparrow}$. The area under the curve $\varrho_s(\lambda, \boldsymbol{\kappa})$ over the bulk band at fixed $\boldsymbol{\kappa}$ is equal to unity until the critical point $\boldsymbol{\kappa}_{\uparrow}$ is reached. At that point the localized symmetrical mode appears, and the weight of the latter vibration increases as the wave vector $\boldsymbol{\kappa}$ increases, reaching its maximum at the point $\boldsymbol{\kappa} = (\pi/2, \pi/2)$.

We note that the system under consideration has no resonance vibrations, and thus has no specific features inside the bulk band.

Briefly, we can state that the behaviour of the PDPS depending on the value of the two-dimensional wave vector (principally, its singularities) is associated with the appearance of localized vibrations in the system. The antisymmetrical vibrations as well as the corresponding features at the edges of the bulk band are described by taking into account explicitly the discreteness of the crystal structure, and thus cannot be shown in principle in the framework of the phenomenological approach. The *exact* functions $\varrho_s(\lambda, \boldsymbol{\kappa})$, $\varrho_a(\lambda, \boldsymbol{\kappa})$ obtained in this paper determine the scattering cross sections of the passive planar defect (interface), and allow us to calculate the contribution of the defect to the thermodynamics of the crystal. Certainly, all of the peculiarities described persist for the interface SH waves described in the framework of the vector model, and can also be treated for the spin waves in magnetically ordered structures.

References

[1] Kosevich Yu A, Syrkin E S and Kossevich A M 1997 *Prog. Surf. Sci.* **55** 59

[2] Farnell G W 1970 *Physical Acoustics* vol 6, ed W P Mason (New York: Academic) p 109

[3] Mutti P, Bottani C E, Ghislotti G, Beghi M, Briggs G A D and Sandercock J R 1995 *Adv. Acoust. Microsc.* **1** 249

[4] Sandercock J R 1978 *Solid State Commun.* **26** 543

[5] Loudon R 1978 *Phys. Rev. Lett.* **40** 581

[6] Loudon R and Sandercock J R 1980 *J. Phys. C: Solid State Phys.* **13** 2609

[7] Bortolani V, Nizzoli F and Santoro G 1978 *J. Phys. F: Met. Phys.* **8** L215
[8] Royer D and Dieulesaint E 1984 *J. Acoust. Soc. Am.* **76** 1438
[9] Stegeman G D and Nizzoli F 1984 *Surface Excitations* ed V M Agranovich and R Loudon (New York: North-Holland) p 195
[10] Toennies J P 1991 *Surface Phonons* ed W Kress and F W de Wette (Berlin: Springer) p 111
[11] Peresada V I 1968 *Fiz. Kondens. Sost. (Kharkov)* **2** 172 (in Russian)
[12] Haydock R 1980 *Solid State Physics* ed H Ehrenreich *et al* (New York: Academic)
[13] Wallis R F, Maradudin A A and Dobrzynski L 1977 *Phys. Rev.* B **15** 5681
[14] Peresada V I and Syrkin E S 1977 *Sov. J. Low Temp. Phys.* **3** 110
[15] Maradudin A A 1981 *Proc. Int. Sch. of Condensed Matter Physics* (Sofia: Bulgarian Academy of Sciences) p 11
[16] Kosevich A M, Syrkin E S and Tutov A V 1996 *Sov. J. Low Temp. Phys.* **22** 816
[17] Kosevich A M, Syrkin E S and Tutov A V 1997 *Proc. 23rd Int. Symp. on Acoustical Imaging* (New York: Plenum) p 513
[18] Mills D L 1992 *Phys. Rev.* B **45** 13 100
[19] Almeida N S, Mills D L and Teitelman M 1995 *Phys. Rev. Lett.* **75** 733
[20] Leibfried G 1955 *Gittertheorie der Mechanischen und Thermischen Eigenschaften der Kristalle* (Berlin: Springer)
[21] Mamalui M V, Syrkin E S and Feodosiev S B 1996 *Sov. J. Solid State Phys.* **38** 3683